Photoprintable Gelatin- graft -Poly(trimethylene carbonate) by Stereolithography for Tissue Engineering Applications

Thomas Brossier, Gael Volpi, Jonaz Vasquez-Villegas, Noémie Petitjean, Olivier Guillaume, Vincent Lapinte, Sébastien Blanquer

Hybrid copolymers based on grafted gelatin-poly(trimethylene carbonate) used in stereolithography towards tissue engineering applications

*Thomas Brossier[a, b], Gael Volpi[b], Jonaz Vasqez-Villegas[c], Noémie Petitjean[c,d], Olivier Guillaume[e], Vincent Lapinte[a], Sébastien Blanquer[a]**

[a] ICGM, Univ. Montpellier, CNRS, ENSCM, Montpellier, France

[b] 3D Medlab, Marignane, France

[c] LMGC, Univ. Montpellier, CNRS, Montpellier, France

[d] IRMB, Univ. Montpellier, INSERM, Montpellier, France

[e] 3D Printing and Biofabrication Group, Institute of Materials Science and Technology, TU Wien Getreidemarkt 9/308, 1060 Vienna (Austria)

ABSTRACT

A new photo-processable hybrid copolymer based on gelatin-poly(trimethylene carbonate) (Gel-*g*-$PTMC_n$) was elaborated and showed a promising potential as resin for stereolithography towards the fabrication of scaffold for tissue engineering. Various lengths of PTMC were grafted from gelatin using hydroxy and amino side groups of the constitutive amino acids. The characterization of resulting hybrid copolymers was fully investigated by quantitative NMR spectroscopy before rendering them photosensitive by methacrylation of the PTMC terminal groups (Gel-*g*-$PTMC_n$-MA). Homogeneous

composition of the photo-crosslinked hybrid polymers was demonstrated by EDX spectroscopy and electronic microscopy. By performing subsequently water absorption,contact angle measurements, and degradation study we also showed the contribution of PTMC amount on the hybrid polymer behavior. The photo-crosslinked materials immersed in water were examined by using tensile experiments and displayed a large panel of materials from hydrogel to elastomer-like. Moreover, the absence of cytotoxicity conducted following the ISO10993 assay, validated the potential of such hybrid polymers in tissue engineering. As proof-of-concept 3D porous objects were successfully fabricated using stereolithography showing the great potential of those hybrid copolymers to be used as scaffolds for tissue engineering and regenerative medicine.

KEYWORDS: Biopolymer, poly(trimethylene carbonate) (PTMC), hydrogel, elastomer-like, stereolithography, grafting-from

---

1. INTRODUCTION

Tissue engineering (TE) is one of the most promising approach for the biomedicine of tomorrow. Most of the TE strategies rely on the use of biomaterials and on their processing to create temporary scaffolding structures. However, despite significant efforts, proposing a universal strategy that could generate an ideal scaffold for tissue engineering remains a considerable gap. Indeed, such scaffolds must not only be biocompatible, biodegradable and porous but must also display sufficient mechanical properties and be endowed with biofunctionalities such as promoting cellular adhesion and proliferation [1]. In that sense one of the crucial steps in the TE strategy is the choice of polymer material. In this context, a broad variety of natural biopolymers and synthetic polymers have been integrated in the composition of TE scaffold [2-3]. More particularly, synthetic-based polymers with specific biodegradability and tunable properties have been extensively used in scaffold production [4-5]. Among them, the family of aliphatic polycarbonates, with the gold standard being poly(trimethylene carbonate) (PTMC), has been largely assessed as scaffold for bone [6], cartilage [7] or intervertebral disc tissue [8]. PTMC is especially recognized i/ for its specific biodegradation by surface erosion, which then does not compromise the mechanical properties during the degradation process and ii/ for its elastomer-like properties, especially upon curing [9]. Moreover, the typical carbonate functions lead to the absence of acidic by-products generated by the degradation of the polymer, which is a huge

advantage in tissue reconstruction [10]. However, despite such promising interest, PTMC remains highly hydrophobic with no cell recognition sites which explains the difficulty for the cells to adhere onto it [11]. In order to overcome those limitations, an attractive approach is to combine such synthetic-based materials with biopolymers originating from the extracellular matrix [12-13]. Biopolymers are widely recognized to be effective matrix for TE scaffolds especially because of their remarkable affinity with water and similarity with the native tissue composition. However, those biopolymers display often weak mechanical properties and their degradation kinetic remains inappropriate to be used as unique component of any scaffolds [14]. Hence, the approach could consist in developing a hybrid polymer based on PTMC to confer suitable mechanical performances and extracellular matrix biopolymers to endow the biomaterials with effective bioactivity. Several biopolymers from extracellular matrix have been already investigated in the reconstructive tissue area including collagen, gelatin, fibrin, elastin and glycosaminoglycan [15-16]. One of the most traditional natural polymers in TE remains the gelatin [17-18]. Gelatin is a protein derived from the denaturation of collagen which then allows to provide favorable cellular bioadhesion due to the numerous RGD sequences. Multiple chemical strategies have been attempted to improve the mechanical properties either by grafting poly(ethylene glycol) (PEG) onto the gelatin [19-20], or else by crosslinking the gelatin via enzymes [21] or by photopolymerization of methacryloyl gelatin (Gel-MA) [22]. But those processes have still limited successes and the achieved mechanical strengths are still far from being suitable. Consequently, the synthesis of hybrid material based on gelatin and PTMC, that will not only reinforce the mechanical properties of the gelatin, but also significantly improve the cell response of the raw PTMC would be of great interest. However, the synthesis of such hybrid materials is challenging, mainly because of the physical and chemical incompatibility between the hydrophobic nature of PTMC and the highly hydrophilic natural biopolymers. Hence, the reported blend approach requires specific conditions to yield homogenous phase and most of the time involved the use of toxic or hazardous solvent [23]. An alternative of the blend approach has been recently reported by Grijpma *et al* that consists in a hybrid network of Gelatin-PTMC obtained from blended methacrylated macromonomer precursors and subsequently photocured [24]. Despite promising mechanical properties, homogeneous dispersion can only be reach by using harsh solvent with a high level of dilution, which then limits the possibility to use such system for scaffold fabrication by additive manufacturing. Unlikely, from another perspective, PTMC has been coupled as hybrid block terpolymer with other type of extracellular matrix such as elastin [25] and

hyaluronic acid [26], in order to generate amphiphilic and self-assembled block copolymers. But grafting directly PTMC on gelatin is an approach never reported so far in the literature, to the best of our knowledge.

We propose here a grafted copolymer by the "grafting from" approach, using TMC monomers and the specific reactive functions of the gelatin as macroinitiator to lead to Gel-g-PTMC$_n$ (Figure 1). In designing and synthesizing such complex materials, a recurrent issue remains the lack of chemical characterizations, which would allow to decipher the individual role of each component to the final behavior of the copolymer structure. Therefore, efforts have been devoted in this work to fully characterize the hybrid material, using several lengths of PTMC grafted from the gelatin. We further functionalized the Gel-*g*-PTMC$_n$ copolymers by inserting photo-sensitive functions in order to generate a photocrosslinked network. We then tested the photocrosslinked hybrid copolymers in terms of mechanical properties, cytocompatibility and degradability. Finally, the photo-sensitive Gel-*g*-PTMC$_n$ copolymers was also develop to validate its processability by 3D printing technology using vat photopolymerization such as the stereolithography (SLA). SLA is recognized for its remarkable efficiency and considerable advantages in terms of versatility in manufacturing, high accuracy and speed [27]. In consequence, we proposed here an attractive option, as it is a versatile and controlled approach, allowing to generate a large variety of hybrid materials based on gelatin and PTMC without any issue of miscibility, and which can be used to fabricate 3D porous scaffolds using SLA.

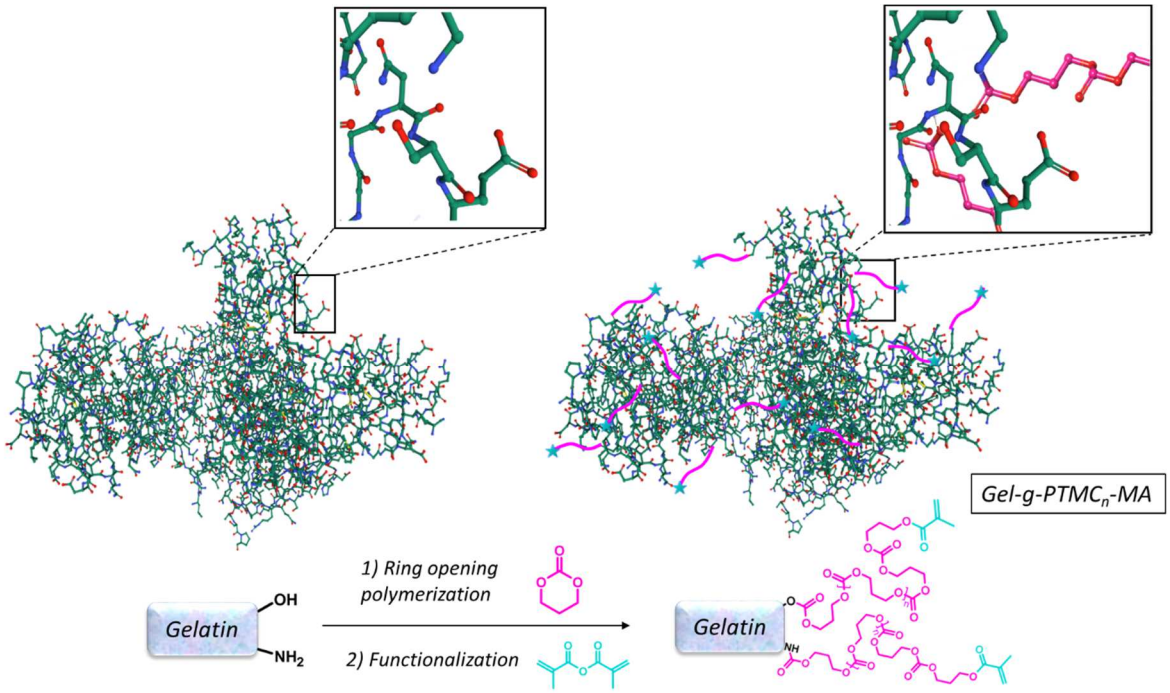

Figure 1. Schematic molecular overview and chemical pathway of the PTMC (pink) grafted from the gelatin and functionalized for further photo-fabrication (blue) (Gel-g-PTMCn-MA).

2. EXPERIMENTAL SECTION

2.1. Materials

Trimethylene carbonate (TMC) was provided by Foryou Medical Devices, China. Gelatin from porcine skin (Type A, gel strength 300 g Bloom), triethylamine (TEA), methacrylic anhydride, hexamethyldisilazane, anhydrous dimethyl sulfoxide (DMSO), dichloromethane (DCM), phosphate-buffered saline (PBS), and 1,5,7-triazabicyclo[4.4.0]dec-5-ene (TBD), stannous octanoate, hexamethyldisilazane were purchased from Sigma Aldrich, France. Darocur 1173 was acquired from BASF (Germany). Orange G dye comes from TCI, Japan. The reagents and solvents were of analytical grade and used as received.

2.2. Characterization and measurements

2.2.1. Nuclear Magnetic Resonance Spectrometry

^{1}H NMR, DOSY NMR and quantitative ^{13}C NMR spectra were recorded on a 400 MHz and 500 MHz Bruker Aspect Spectrometer. $CDCl_3$ and D_2O were used as deuterated solvent. Chemical shifts were given in parts per million (ppm). The reference peaks were residual D_2O at 4.79 ppm for ^{1}H NMR or,

$CDCl_3$ at 7.26 ppm and 77 ppm for ^{13}C NMR. Conversion was also determined by ^{1}H NMR spectroscopy. Degree of polymerization (DP_n) was calculated from quantitative ^{13}C NMR according to the following equation (1).

$$DPn = \frac{\int c_{62ppm/2}}{\int c_{59ppm}} \qquad (1)$$

2.2.2. Degree of swelling

The water uptake of the Gel-*g*-$PTMC_n$ was investigated. Photo-crosslinked polymers were prepared and weighted after irradiation to obtain the initial mass (mi). Then, polymers were leaved in distilled water for 24 h and water was renewed five times. After swollen, the polymers were weighed to determine the swollen mass (ms) and vacuum-dried to determine the dry mass (md).

The photo-crosslinking efficiency was calculated by the gel content (2) and the water absorption was determined by the equilibrium water content (EWC) (3).

$$\text{Gel content} = \frac{md}{mi} * 100 \qquad (2)$$

$$\text{EWC} = \frac{ms-md}{ms} * 100 \qquad (3)$$

2.2.3. Complex Viscosity

Gel-*g*-$PTMC_n$ polymers were diluted in DMSO at 20 wt%. The viscosity properties were investigated by performing complex viscosity measurements. Viscoelastic properties of Gel-*g*-$PTMC_n$ solutions were measured using a rheometer apparatus (Physica Modular Compact MCR301, Anton Paar, Germany) at frequencies ranging from 0.1 to 10 Hz (0.6 to 62.8 rad·s^{-1}) at 25 °C. Oscillatory shear measurements were conducted using a 40 mm 2° diameter steel cone with a truncation gap of 55 µm to measure the complex viscosity (η^*) and deduce the zero-shear viscosity (η_0) at 0.1% strain.

2.2.4. Contact angle

Contact angle measuring instrument (G10 optical, Krüss, Germany) was used to determine the surface tension of Gel-*g*-$PTMC_n$ network films. Contact angle was measured on water drops deposited on 3 different areas of the surface with a microsyringe.

2.2.5. Scanning electronic microscope and energy-dispersive X-ray spectroscopy

The surface elemental compositions of Gel-*g*-PTMC$_n$ network films were determined using scanning electronic microscope (SEM) (Phenom-world ProX) coupled with an energy-dispersive X-ray spectroscopy (EDX) using an accelerating voltage of 15kV. Mapping quantification analysis was performed using the dedicated thermo Scientific Phenom Elemental Mapping Software. Results are given in % of atomic element. SEM images was performed on freeze-dried films and sputter-coated with gold.

2.2.6. Mechanical measurements

Elongation at break and Young modulus of Gel-*g*-PTMC$_n$ network samples were measured with an Instron3366L5885 tensile tester using dumbbell samples (ISO527-2) immersed in water. The cross-head speed was 5 mm.s^{-1}. The elongation at break was expressed as a percentage of the original length and the modulus was obtained at 0.5% of deformation by stress/strain.

2.2.7. Crosslinker chamber and building of 3D structures with stereolithography apparatus

Films were photo-crosslinked in UV Crosslinker Biolink chamber (Thermo Fisher, France) for 10 min at 100 J/cm² using 365 nm wavelength at 10 cm from the surface of the specimens, at room temperature.

Cubic 3-dimensional porous structures with an average pore size and strut of 1 mm were designed using STL format from Rhinoceros 3D. The 3D structures were built from the above-mentioned resins by stereolithography (SLA) using a digital light processing (DLP) apparatus (Asiga Max X27, Australia). The 3D objects were constructed in the DLP apparatus by photo-crosslinking subsequent layers of resin with thicknesses of 100 µm, upon which a pixel pattern is projected. Each layer was illuminated at an intensity of 20 mW/cm² for 30 s. After building, the structures were washed with DMSO and extracted for 72 hours with DCM to leach out DMSO. The final structures were dried after 2 days at room temperature or swelled in water.

2.2.8. Evaluation of cytotoxicity of the crosslinked polymers

Cytocompatibility of the different Gel-*g*-PTMC$_n$ networks (with increasing percentage of PTMC, from DP$_6$ to DP$_{32}$) was tested via extraction tests in accordance to the ISO 10993-5 guidelines in order to detect the presence of cytotoxic compounds released from the samples into the media.

The extract tests were conducted by immersing crosslinked copolymer disks (surface area: 1.25 cm^2 mL^{-1}) in extraction vehicle, consisting on cell culture medium, i.e. high glucose Dulbecco's modified Eagle medium (HG-DMEM, Gibco, United Kingdom) supplemented with 10% newborn calf serum (NCBS) and 1% penicillin-streptomycin. This incubation was conducted at 37 °C for 3 days. Next, the extracts were collected and used as feeding media for L929 fibroblasts.

The L929 fibroblasts were seeded at a density of 5.0 x 103 cells $well^{-1}$ in 96-well plates and cultivated until reaching approximately 70% confluency. Next, the culture medium was removed and the cells were incubated in 100 µL of the extracts for 24h (n=6). Extract-free HG-DMEM was applied as feeding medium for the cells as positive controls whereas culture medium supplemented with 5% DMSO was applied as feeding medium for the cells as negative control.

The metabolic activity of the L929 fibroblasts was assessed using PrestoBlueTM Cell Viability Reagent (Invitrogen, Fisher Scientific, Vienna, Austria) at 24h of the culture. The fluorescence of the medium was recorded (λ_{ex} = 560 nm; λ_{em} = 590 nm) using a plate reader (SynergyTM H1 BioTeKTM plate reader, Bad Friedrichshall, Germany). The fluorescence value obtained for the cells cultivated in extract-free Medium was considered as 100% viability for each time point. The fluorescence values of the sample extracts were normalized against the corresponding control group and expressed relative to this 100% viability. Morphology of the cells spreading onto the plastic of the 96 wp were observed by taking images after the extract test, using bright field imaging of the LSM700 (Zeiss, Germany), mag. 20 (Camera AxioCam 105).

Morphology of the cells spreading directly onto the surface of the Gel-*g*-$PTMC_n$ was observed by seeding 10.0 x 103 cells of L929 / film (2 mm thick, 10 mm diameter). After 3 days of incubation in HG-DMEM supplemented with 10% NCBS and 1% penicillin-streptomycin, the samples were retrieved for Scanning Electron Microscopy observation (SEM Philips XL Series 30). Briefly, samples were washed in PBS, fixed in buffered paraformaldehyde at 4%, followed by gradual dehydration in ethanol and by immersion in hexamethyldisilazane. After drying, the samples were sputter-coated with Au and investigated by SEM.

2.2.9. Degradation study

In vitro degradation of the PTMC networks was evaluated in harsh condition in order to accelerate the degradation process. Cylindrical photocrosslinked specimens (1 cm diameter) with an approximate

thickness of 2 mm were placed in NaOH 1M solution at 40°C. Before and after 4h, 6h and 8h of incubation, specimens were collected, wiped and deposited on glassplate to visualize the degradation.

2.3. Synthesis and formulation

2.3.1 Synthesis of gelatin methacrylate (Gel-MA).

Gel-MA was synthesized according to the previously published method [28]. Briefly, 10 g of porcine gelatin type A (0.015 mol, 1 eq.) was dissolved in 200 mL of PBS under continuous stirring at 50 °C. Then, methacrylic anhydride (0.06 mol, 4 eq.) and triethylamine (0.06 mol, 4 eq.) were added to the solution dropwise. The reaction was stirred vigorously at 50 °C for 2 h. The solution was then dialyzed against deionized water using a dialysis tubing (cutoff: 8 kDa) at 50 °C for one week to remove salts and unreacted methacrylic anhydride. The Gel-MA solution was freeze-dried resulting in porous Gel-MA foam stored until used.

2.3.2. Synthesis of PTMC by ring opening polymerization.

The synthesis of 50 g of PTMC (Mn = 10 000 g/mol) was carried out by ring-opening polymerization of TMC (0.49 mol, 100 eq.), initiated by 1,6-hexanediol (0.0049 mol, 1 eq.) and catalyzed by stannous octanoate at 130 °C (0.05 wt%) for 24 hours under inert N_2 gas. After cooling to room temperature, the PTMC was dissolved in dried dichloromethane (50 mL) and precipitated in cold methanol. The precipitate was filtered and dried in the dark at ambient conditions overnight.

2.3.3. Synthesis of grafted PTMC from the gelatin (Gel-g-PTMC$_n$)

Gel-*g*-PTMC$_n$ was carried out *via* ring-opening polymerization in solution. Briefly, gelatin was charged in a round-bottom flask under inert nitrogen atmosphere and dissolved in dry DMSO. The solution was stirred at 50 °C until full gelatin dissolution. Then addition TMC monomer was performed. The mixture was stirred at 50 °C until complete consumption of the free amino pendant groups as described to our previous research [29]. Then TBD catalyst was added to run the full polymerization. The reaction mixture was stirred at 50 °C under inert nitrogen atmosphere and followed by ^{1}H NMR spectroscopy until full conversion. After the reaction was completed, the crude was precipitated into water and washed with ethanol. Exception was done for the determination of

ROP initiation where the reaction was stopped just after the beginning of the polymerization, then purified by dialyze and analyzed by ^{1}H NMR spectroscopy in D_2O.

2.3.4. Synthesis of PTMC and methacrylated Gel-g-PTMC$_n$ (Gel-g-PTMC$_n$-MA)

PTMC and Gel-*g*-PTMC$_n$ were end-functionalized with methacrylate groups using methacrylic anhydride (4 eq.) in the presence of triethylamine (4 eq.) in dichloromethane (50 wt%). For all the formulations, the solution was then stirred in the dark for 3 days at room temperature under a nitrogen atmosphere. The mixtures were precipitated in cold ethanol. The precipitates were filtered and dried in the dark at ambient conditions overnight. The final product was stored at 4 °C until used.

2.3.5. Formulation of stereolithography resins

To prepare resin formulations for SLA, Gel-*g*-PTMC$_n$ was mixed with DMSO (40 wt%) as a non-reactive diluent. Darocur 1173 (3 wt% relative to polymer) and Orange G (0.2 wt% relative to polymer) were added as photoinitiator and dye agent, respectively.

3. RESULTS & DISCUSSION

3.1. Grafting-from strategy

By definition, the term of covalent grafting on polymers is applied to define one of the three following grafting methods: “grafting-to”, “grafting-through” and “grafting-from”. In this work we proposed to focus on the “grafting-from” where the graft copolymers will grow *in situ* from the active functions of the initial backbone polymer. In comparison to other methods, hybrid polymers obtained by grafting-from approach lead to highly ramified grafted copolymers because of the polymer–monomer reaction, which is less affected by steric hindrance than other the polymer–polymer reactions. Moreover, the purification steps are remarkably simpler as the separation of the resultant grafted copolymers from unreacted monomer precursors can be easily done by precipitation. However, grafting-from remains rarely employed especially because of the difficulty of characterizing the ratio of grafted copolymer. Such observation is even more true in the case of amphiphilic copolymers, especially due to the incompatibility between the blocks, which renders the characterization complex. Therefore, the synthesis of hybrid copolymers using grafting-from strategy makes sense if the grafting can be controlled with an efficient and easy to conduct characterization procedure. We therefore

particularly focused this work on the characterization procedure in order to prove the efficiency of the grafting and to determine the proportion of TMC grafted from the gelatin.

PTMC grafting from the gelatin has been done by ring opening polymerization (ROP) of the monomer TMC from the specific active functions on the gelatin susceptible to initiate ROP. Consequently, all amino acids exhibiting a pendant alcohol function can be involved in the initiation of ROP. Moreover, we recently demonstrated that amino groups were also able to initiate ROP for TMC, which then generates urethane functions [29]. Therefore, the amino acids susceptible to initiate the ROP of TMC from the gelatin might be serine (0.328 mmol/g), threonine (0.144 mmol/g), hydroxyproline (0.902 mmol/g), lysine (0.259 mmol/g), and hydroxylysine (0.066 mmol/g) [30-32](Figure 2).

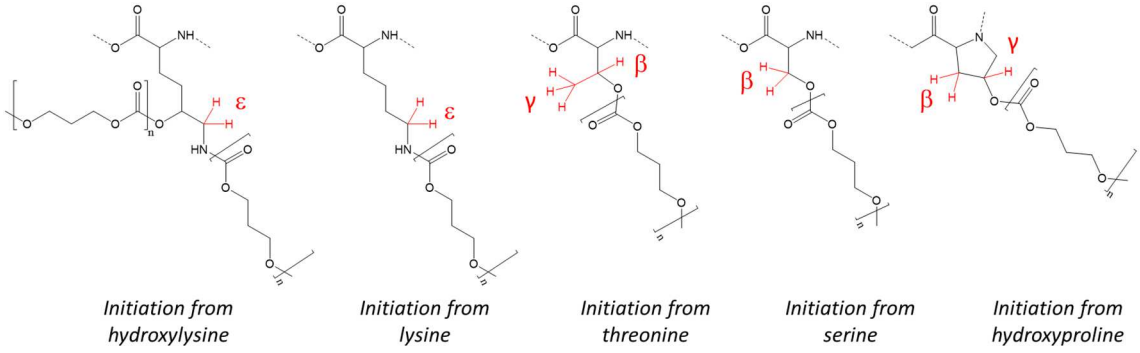

Figure 2. The resulting chemical structure after ROP of TMC from amino acids of the gelatin.

In the perspective to avoid the presence of residual metal in the final material, we decided to ban metallo-catalysts and oriented the study toward organo-catalysts in particular nucleophilic catalysts such as TBD. To prevent any gelatin degradation, the TBD reaction was conducted at low temperature [33]. ROP of TMC using TBD catalyst has already been investigated with alcohol [34-35] or amine group initiation [29], even though the later one requires multiple steps. Indeed, previous work demonstrated that the ROP with TBD initiation by amine groups must be done in two successive steps, the first being the ring opening of one TMC unit in absence of catalyst followed by classic ROP initiated by the generated hydroxy groups [36]. Therefore, the ROP initiation of TMC was activated from the alcohol and amine functions of the gelatin. Finally, it is also crucial to not neglect the type of solvent that will be used, as it must be able to solubilize the gelatin, the TMC monomers and the resulting hybrid polymer. DMSO was selected to perform the ROP of the TMC as this solvent fulfill

these requirements, and further DMSO is recognized as being low hazardous solvent, in contrast to the traditional solvent used for hybrid copolymers.

Table 1. Chemical shift of characteristic peaks from the amino acids involved in ROP initiation

Characteristic proton of the amino acids involved in ROP initiation	Amino acid abbreviation	Chemical shift of protons before ROP (ppm)	Chemical shift of protons after ROP (ppm)
γ-Threonine (CH_3)	γ-Thr	1.2	1.5
β-Threonine (CH)	β-Thr	4.3	5.4
β-Serine (CH_2)	β-Ser	3.9	4.1
ε-Hydroxylysine (CH_2)	ε-Hyl	3.0	3.3
ε-Lysine (CH_2)	ε-Lys	3.0	3.3
γ-Hydroxyproline (CH)	γ-Hyp	4.6	5.5
β-Hydroxyproline (CH_2)	β-Hyp	2.4	2.6

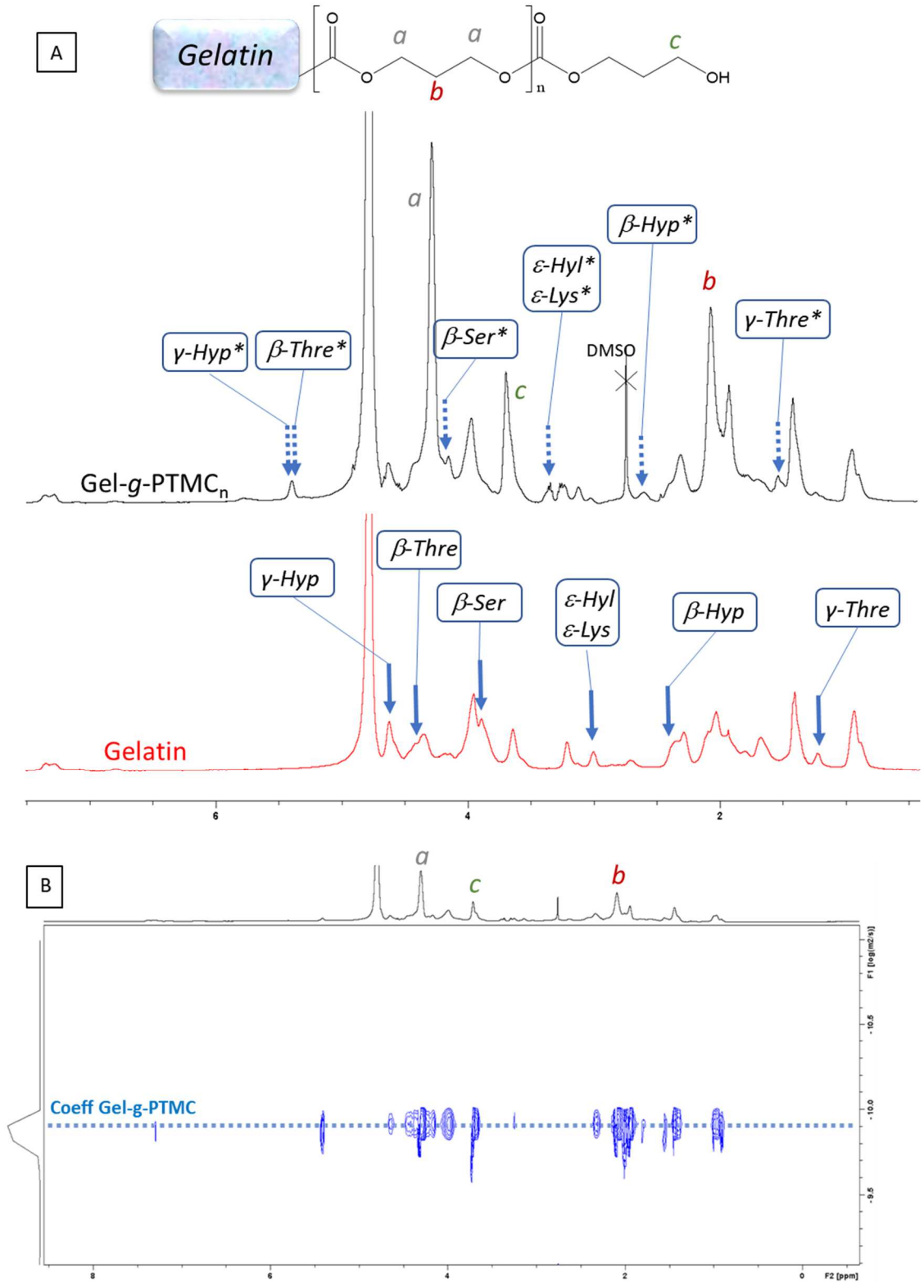

Figure 3. D_2O ^1H NMR spectra of native gelatin and Gel-*g*-$PTMC_n$ (A), with full line arrows to show the characteristic peaks of the amino acids involved in the ROP from the gelatin and dot line arrows and asterisks for the modified amino acids from Gel-*g*-$PTMC_n$ (Table 1); D_2O DOSY NMR spectrum of Gel-*g*-$PTMC_n$ (B).

Several ratios of PTMC have been synthesized, and the reaction yields reached in average 92±4 % for all the hybrid polymers, which then indicates the high performance of the reaction. It can be noticed that the physico-chemical behavior of the resulting materials, especially the solubility, differs with the proportion of PTMC, which will then result in serious issue for the characterization. Therefore, to get a global and correct characterization of the grafting, a diagonal approach was undertaken using first the ^{1}H NMR in D_2O to validate the ROP initiation from the gelatin while a quantitative ^{13}C NMR spectroscopy in $CDCl_3$ was used to determine the proportion of grafted PTMC.

3.1.1 Validation of ROP initiation from gelatin using ^{1}H NMR in D_2O

^{1}H NMR spectroscopy in D_2O has been used to determine the initiation process of the TMC from the gelatin. Indeed, D_2O was the most appropriate solvent to characterize the gelatin with well-defined and attributed characteristic protons of amino acids, especially those involved in the ROP initiation (Figure 3). Therefore, in order to keep solubility in water, the analyses in D_2O must be perform at the beginning of the polymerization when the TMC starts to be initiated by the active functions of the gelatin.

From the ^{1}H NMR spectrum of the gelatin, the characteristic peaks of the amino acids involved in the ROP initiation (serine, threonine, lysine, hydroxylysine and hydroxyproline) were assigned (Figure 3 and Table 1). Upon polymerization of the TMC monomers, the characteristic peaks from such amino acids shifted, which proved the grafting (Figure 3A, Table 1). Based on the study from Claassen et al. on methacryloyl gelatin [30], it has been possible to assign each shifted peak attributed to the modified amino acids, once the polymerization initiated. Such peak shifting can be also correlated with the growing signal of the characteristic peaks from the PTMC polymer at 2 and 4.2 ppm. Moreover, to ensure the grafting of PTMC on the gelatin, a DOSY-NMR analysis in D_2O has been performed. In Figure 3B, the single diffusion coefficient demonstrated the presence of both gelatin and PTMC within the same macromolecule and consequently the success of the grafting-from approach for the synthesis of hybrid polymers. However, it must be noticed that in return, quantitative ^{13}C NMR spectroscopy of grafted gelatin in D_2O is not sufficiently consistent because of the high complexity of the spectra, and the determination of the grafted PTMC ratio cannot be identified as far as the hybrid copolymer remains soluble in water.

3.1.2 Quantification of grafted PTMC by quantitative ^{13}C NMR spectroscopy in $CDCl_3$

Even though the quantification in D_2O was not possible, ROP initiation from the gelatin was successfully demonstrated. Therefore, it was relevant for us to reach higher ratios of PTMC and potentially be able to quantify the grafting. However, the threshold of solubility from water to organic solvent is narrow, and the Gel-*g*-$PTMC_n$ becomes rapidly insoluble in water once PTMC chains are growing. Consequently, the gelatin fraction being non soluble in organic solvent, only the PTMC blocks from the copolymer was visualized by NMR spectroscopy in $CDCl_3$ using the different Gel-*g*-$PTMC_n$. We investigated the potential of quantitative ^{13}C NMR spectroscopy to measure the average size of grafted PTMC from the gelatin. As shown in Figure 4A, the end-chains are easily distinguishable at 59 ppm while the peak at 62 ppm represents the aliphatic carbons of the PTMC chain, and at 154 ppm the carbon of the carbonate functions. By comparing the peak intensity using the equation (1), the number of TMC grafted from the gelatin can be calculated and the average chain size of PTMC can be subsequently deducted. As schematized in Figure 1, gelatin is a huge protein compared to the PTMC chains and therefore we chose a nomenclature which takes into consideration the different ratio of PTMC regarding their DP_n rather than the ratio of PTMC related to gelatin. We determined four different grafting ratios named: Gel-*g*-$PTMC_6$; Gel-*g*-$PTMC_{10}$; Gel-*g*-$PTMC_{16}$ and Gel-*g*-$PTMC_{32}$. It is crucial to mention that the conversion rates measured by ^1H NMR spectroscopy were around 93±2 % for all the synthesized Gel-*g*-$PTMC_n$. Consequently, the high degree of conversion with satisfying yield of reaction coupled with the DOSY-NMR spectroscopy can ensure that all the TMC were grafted on the gelatin.

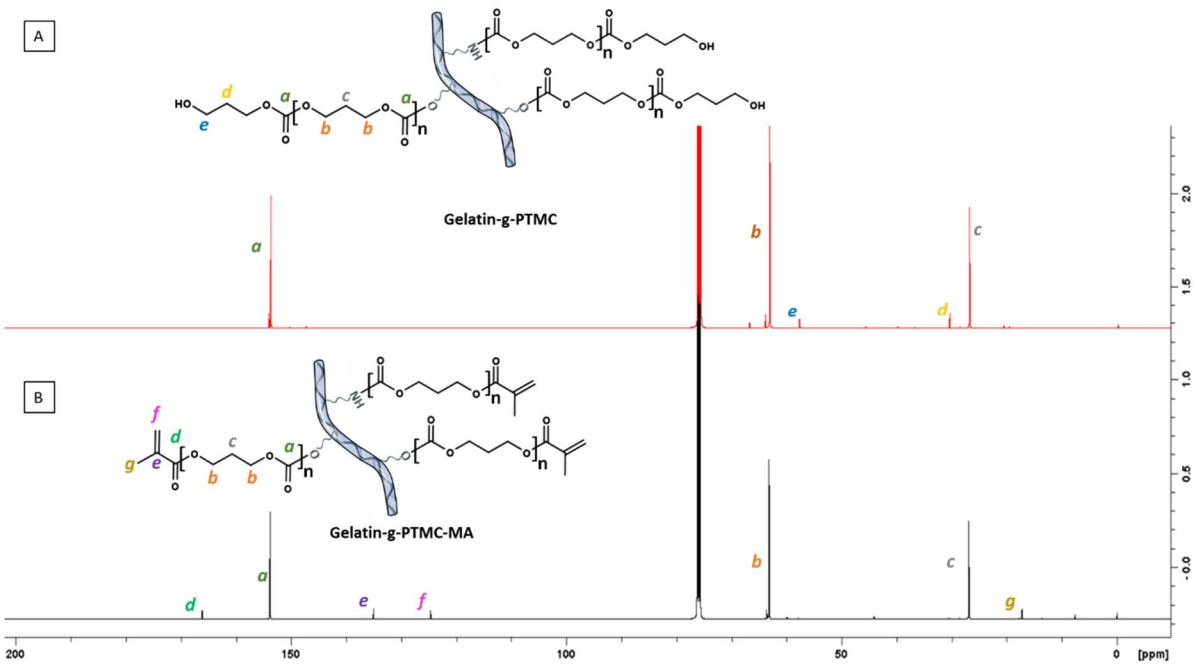

Figure 4. Quantitative ^{13}C NMR spectrum of Gel-*g*-$PTMC_n$ (A), and after methacrylation Gel-*g*-$PTMC_n$-MA (B) in $CDCl_3$.

Finally, the last step to obtain photosensitive polymers for SLA fabrication consists in the functionalization of the hybrid polymers by methacrylate active moities. This approach is now widely used and recognized to be efficient to lead to photo-crosslinkable polymers [37]. The functionalization was followed by quantitative ^{13}C NMR spectrometry with the apparition of the characteristic signal of the carbonyl from the grafted methacrylate at 168 ppm (Figure 4B). The proportion of methacrylate has been calculated by comparing the characteristic peaks of the methacrylate carbonyl with those of the carbonyl from the PTMC chains at 152 ppm. For all the hybrid polymers we reached an average of 80±3% of grafted methacrylate functions.

The rheological viscosity measurements in DMSO were monitored on Gel-*g*-$PTMC_n$ samples in order to determine the influence of the length of PTMC chains grafted on gelatin backbone. This characterization is essential for our application, as it is well-known that the viscosity is a leading parameter for further stereolithography processing. As shown in Figure S1, the Gel-*g*-$PTMC_n$ viscosity was not dependent to the frequency by contrast to the native gelatin. The grafting of PTMC on the gelatin biomacromolecule stabilized the rheological behavior in frequency as pristine PTMC. Moreover, higher the DP_n of the PTMC is, higher the viscosity is, ranging from 0.24 to 136.7 MPa.s

for DP_6 and DP_{32}, respectively. The viscosity depended highly on the ramifications of macromolecular structure, and consequently an exponential enhancement of the viscosity can be noted, which corroborates the proportion of PTMC calculated by NMR. The presence of longer PTMC chains increases the chain entanglement, which then amplifies the viscosity of the resin.

3.2. Physical properties of photo-crosslinked hybrid copolymers Gel-g-$PTMC_n$

The photosensitive hybrid polymers Gel-*g*-$PTMC_n$-MA was then successfully photo-crosslinked in a UV crosslinker chamber at 365 nm after 10 minutes in DMSO (20 wt%) in presence of photo-initiator Darocur 1173 at room temperature. The complete consumption of the photoreactive methacrylate units has been checked by FT-IR spectroscopy regarding the characteristic C=C band at 1640 cm^{-1} (data not shown). The network materials were characterized by various technics to demonstrate the impact of PTMC on gelatin on both the surface and the inner part of films from the resulting materials.

Table 2. Characteristics of photo-crosslinked Gel-*g*-$PTMC_n$

	Nitrogen[a] **%**	**θ** (°)	**Gel content[b]** **%**	**Water uptake[c]** **%**
Gelatin	26±0.6	54±1.5	70.9±0.5	71.2±0.4
Gel-*g*-$PTMC_6$	10±1.1	65±5.1	81.9±0.6	8.7±0.7
Gel-*g*-$PTMC_{10}$	5±0.1	81±2.7	89.6±1.4	3.8±1.1
Gel-*g*-$PTMC_{16}$	4±0.7	90±1.7	90.9±0.8	2.4±0.5
Gel-*g*-$PTMC_{32}$	2±0.5	95±4.7	97.3±2.2	2.2±0.4
PTMC	0	104±2.1	95.9±1.1	1.3±0.2

[a]: Determined by mapping quantification using EDX, [b]: Determined with the equation (2), [c]: Determined with the equation (3)

First of all, the photo-crosslinking density was determined by the measurement of gel content (Table 2). It appears that for grafted PTMC above DP_{10} the networks were formed with gel content between

81 and 95 % in DMSO. In contrast, for gelatin and Gel-*g*-PTMC$_6$ the gel content is lower due to the limited solubility of the gelatin in DMSO, which then may favor intramolecular curing.

The only moiety of the hybrid Gel-*g*-PTMC$_n$ bearing nitrogen atoms is the gelatin. Consequently, the percentage of nitrogen can be an efficient probe to estimate the amount of gelatin in Gel-*g*-PTMC$_n$ network. The SEM images were undertaken on the Gel-*g*-PTMC$_n$ film after cross-section in order to access to the inner part of the materials (Figure S2), and no observation of phase separation can be visualized. The chemical homogeneity of the samples was then determined by SEM-EDX analysis (Figure 5A) for nitrogen investigation. Firstly, as shown in the mapping quantification, similar amounts of nitrogen were detected in different points of each Gel-*g*-PTMC$_n$ network film demonstrating the homogeneous distribution of the gelatin for each hybrid copolymers - without phase segregation. Secondly, as expected the proportion of nitrogen decreased when the length of PTMC chain in Gel-*g*-PTMC$_n$ network increased, as shown in Table 2. Interestingly, such evolution is proportionately following the same trend of the DP$_n$ from the grafted PTMC.

The Gel-*g*-PTMC$_n$ network composition also influenced the hydrophilic behavior of the films, as illustrated by contact angle measurement (Figure 5B). We noted a round drop on the surface of pristine photo-crosslinked PTMC and Gel-*g*-PTMC$_n$ with PTMC chains above DP$_{10}$. The values were closed to 100°, typical value of a hydrophobic surface. By contrast, for pure gelatin or Gel-*g*-PTMC$_6$ network, the contact angle decreased to 55-65° with a spread drop on the surfaces (Table 2). The regular increase of contact angle value with the length of the PTMC chains demonstrates the hydrophobization of surface along with the PTMC content.

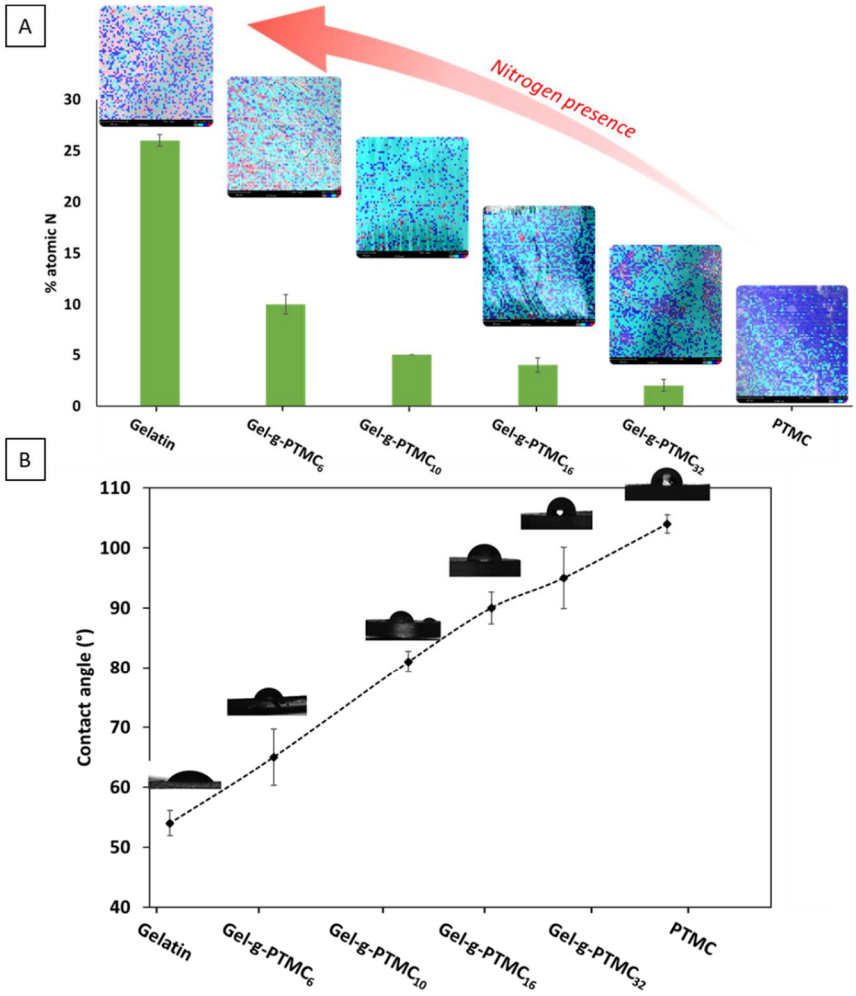

Figure 5. Nitrogen amount of photo-crosslinked film´s cross-sections analyzed by SEM-EDX (red for nitrogen, blue for oxygen, green for carbon) (A) and contact angle on Gel-*g*-PTMC$_n$ surface (B).

The hydrophilic behavior of such hybrid polymers is crucial to foresee any tissue engineering applications. Hence, in correlation with the contact angle measurements, the capacity of the Gel-*g*-PTMC$_n$ networks to absorb water was determined by the water uptake study (Table 2). The Gel-*g*-PTMC$_n$ network values were gathered into the region from 2.2% to 8.7%. As expected, the most hydrophilic materials, owned to the highest water uptake value were the pure photo-crosslinked gelatin and the Gel-*g*-PTMC$_n$ bearing the shortest PTMC chains. In contrast, pure photo-crosslinked PTMC and Gel-*g*-PTMC$_n$ bearing the longest PTMC chains exhibited more hydrophobic properties. Despite a non-neglected water uptake, the samples do not swell in water which can be considered as a favorable parameter for our targeted application. Indeed, materials that do not swell in water have reduced risks of deformation and more stable mechanical properties.

3.3. Mechanical properties of hybrid materials Gel-g-PTMC$_n$ network

The tensile test experiments, in immersed water, were realized on the photo-crosslinked PTMC and gelatin samples as well as on Gel-*g*-PTMC$_n$ networks (Figure 6 and Table 3). As reported in literature, the singular behavior of crosslinked gelatin (low elongation at break, 18% and maximum stress, 0.16 MPa)[38] contrasted with crosslinked PTMC (higher elongation at break, 327% and maximum strain, 1.53 MPa)[39-40]. Our results corroborated such findings. For the Gel-*g*-PTMC$_n$ network, the values ranged in a region between the properties of the gelatin and PTMC, and it can then be identified an evolution of the properties that are following three distinct trends.

First of all, already for Gel-*g*-PTMC$_6$ network the mechanical properties are substantially improved compared to photo-cured gelatin in terms of maximum stress and elastic modulus. Then, by increasing the degree of polymerization of grafted PTMC, the Young modulus starts to significantly decreases while the maximum stress and strain increase. Hence, 13% of elongation at break was measured for short PTMC chains whereas 96 % was reached for DP$_{32}$ of PTMC (Table 3). Finally, Gel-*g*-PTMC$_{32}$ network tends to become softer and more elastic, with the elastic modulus falling down to 0.95 MPa and the stress at break down to 0.48 MPa. This typical evolution can be correlated with the mechanical properties of photo-crosslinked PTMC homopolymer, where low molecular weights are rather stiff with low elongation, while the elasticity increases with higher degree of polymerization [40]. Interestingly, between Gel-*g*-PTMC$_{10}$ and Gel-*g*-PTMC$_{16}$ network, low evolution of the mechanical properties is visible, which means that it may exist a threshold of PTMC length where the mechanical properties are stable and others where it significantly progresses. These results demonstrated the relevance of the association between gelatin and PTMC by grafting while they are both immiscible.

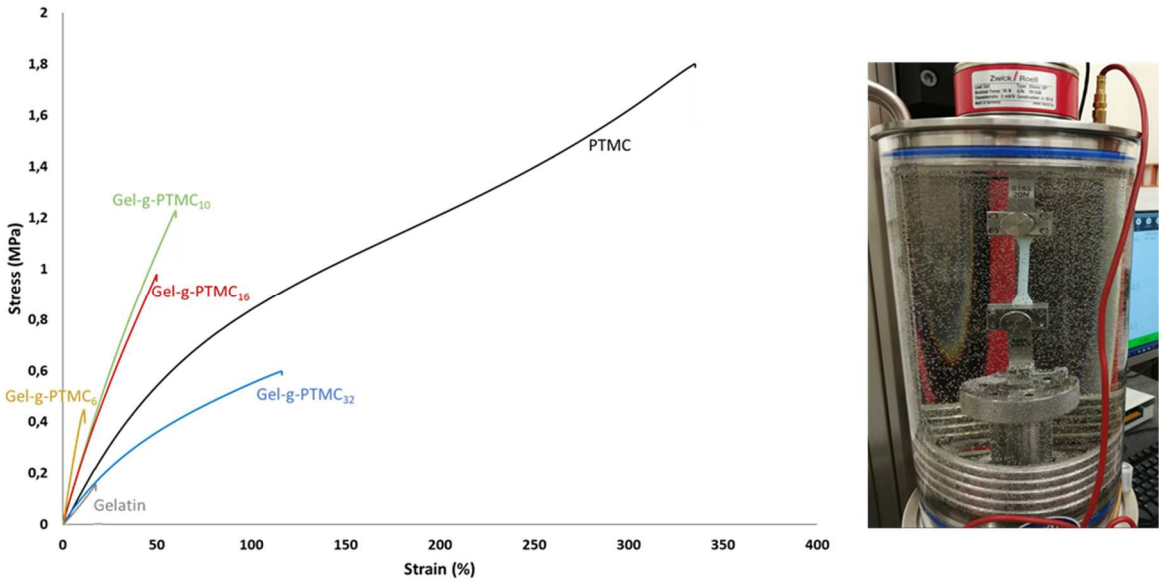

Figure 6. Mechanical properties of photo-crosslinked gelatin, PTMC and the hybrid copolymer Gel-*g*-PTMC$_n$ with increasing DP$_n$ values.

Table 3. Mechanical properties of hydrated photo-crosslinked gelatin, PTMC and Gel-*g*-PTMC$_n$

	σ_{max} (MPa)	ε_{max} (%)	Young modulus (MPa)
Gelatin	0.16±0.03	18.63±3.96	0.74±0.13
Gel-*g*-PTMC$_6$	0.52±0.18	13.73±3.75	4.62±0.84
Gel-*g*-PTMC$_{10}$	1.07±0.14	52.96±8.12	2.76±0.20
Gel-*g*-PTMC$_{16}$	1.19±0.04	59.58±0.46	2.43±0.05
Gel-*g*-PTMC$_{32}$	0.48±0.06	96.39±16.10	0.95±0.09
PTMC	1.53±0.29	327.30±6.89	1.29±0.17

3.4. Cytocompatibility of the hybrid polymer network Gel-g-PTMC$_n$

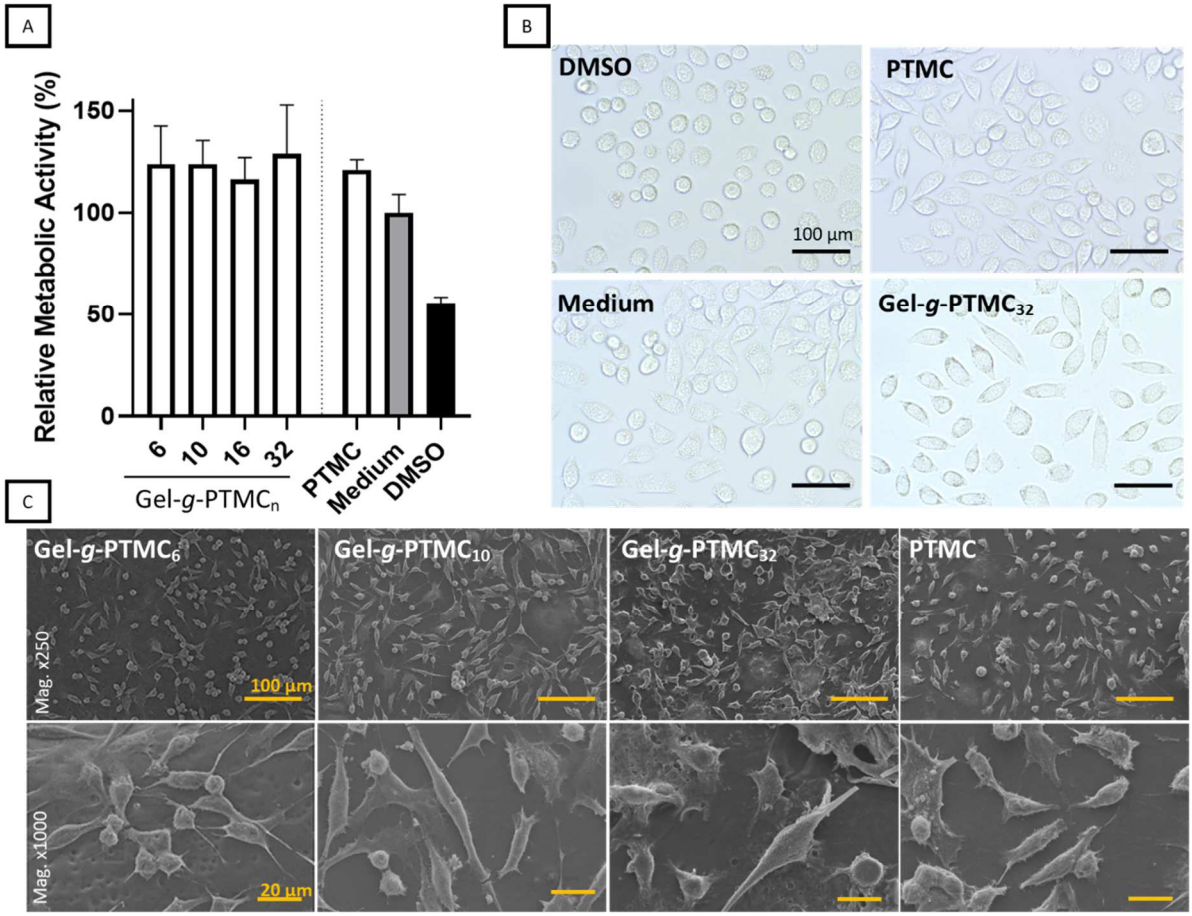

Figure 7. *Indirect cytotoxicity assay:* Relative metabolic activity of L929 fibroblasts cultured in sample extracts or extract-free media for 24 hours. Ctrl (+) is extract-free medium and Ctrl (-) is culture medium supplemented with 5% DMSO as negative control group. The statistical analysis, performed by one-way ANOVA with Tukey post-test, with $p < 0.01$ n=6, did not show any differences when comparing Ctrl (+) to extract media (A). The morphology of the fibroblasts L929 was similar after incubation with the different extracts (B). *Direct cytotoxicity assay*: SEM images of the cells proliferating onto the films of Gel-*g*-PTMC$_n$ mag 250 (top row) and 1000 (bottom row) (C).

Gelatin and PTMC are both biocompatible polymers and have been approved by Food and Drug Administration in various applications. However, the chemical modification applied to obtain photopolymerizable Gel-*g*-PTMC$_n$ might induce potential adverse effects on cell viability (e.g. leachable chemical substances). In order to detect possible leachable cytotoxic compounds, we performed an extract test according to ISO 10993-5. Figure 7A represents the relative metabolic activity of L929 fibroblasts that were cultured in the extracts of Gel-*g*-PTMC$_n$ with increasing amount of PTMC, normalized against medium (ctrl +). The extractions performed in cell culture medium revealed no significant adverse effect on the viability of L929 fibroblasts up to 72h of the culture for

any of the applied materials. Ctrl (-) based on 5% of DMSO showed sign of cytotoxicity as a reduction of the metabolic activity of the L929 of 45% was detected. The morphology of the fibroblasts that were cultured in sample extracts were similar to those of the positive control group, and exhibited a spreading phenotype. Once more, cells incubated with 5% DMSO exhibited a distinct behavior, with a significantly more pronounced round-like morphology, sign of cytotoxicity (Figure 7B).

A direct cytotoxicity assay was performed by directly seeding the fibroblasts onto the Gel-*g*-PTMC$_n$ films (Figure 7C). After 72 hours of proliferation, all the groups allowed cells to adhere and to colonize the surface of the films, independently of their chemical composition. The morphology of the adhering cells is similar, with numerous filopodia and extensive cytoplasmic elongation. Mitotic cells are distinguished in all the groups, which supports of compatible nature of the biomaterials.

Overall, the cytocompatibility tests confirmed that the newly Gel-*g*-PTMC$_n$ are compatible. No significant differences were observed between the groups with various PTMC length, neither in adhesion nor in proliferation. Further analyses are required to assess if the presence of gelatin further strengthen the cell adhesion as we hypothesized, due to the presence of RGD motif in gelatin, absent in PTMC.

3.5. Degradation study of the hybrid polymer network Gel-g-PTMC$_n$

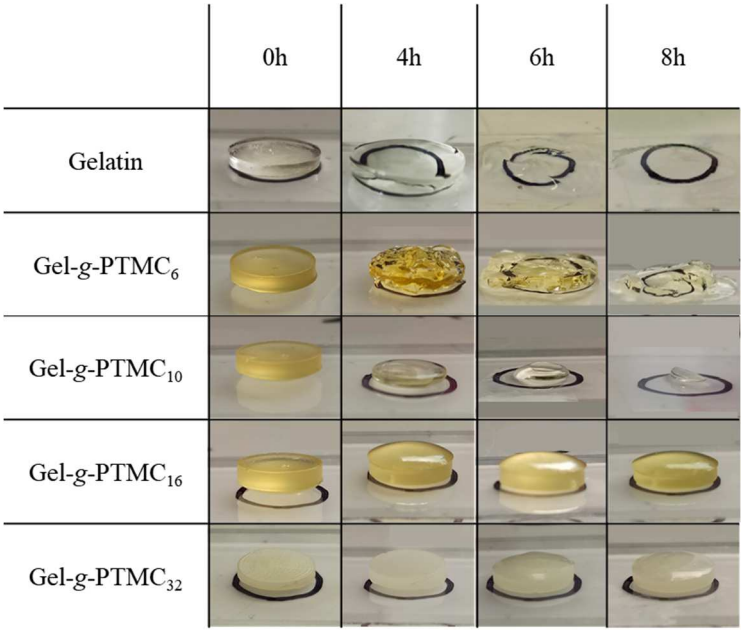

Figure 8. Pictures of the degraded Gel-*g*-PTMC$_n$ and gelatin networks at time incubation time points in a solution of NaOH 1M at 40°C.

To determine the degradation mechanism, we performed a preliminary study using an accelerated degradation condition. The degradation studies were evaluated on cylindrical samples based on photocrosslinked Gel-*g*-PTMC$_n$ and photocrosslinked gelatin (Figure 8). Interestingly, the degradation behavior of each grafted PTMC was different. Copolymers with the lowest amount of PTMC (Gel-g-PTMC6) behave similarly to photocrosslinked gelatin, which typically tend to swell after 4h, then collapse after 6h. Such initial swelling behavior can be explained by the size of the network meshes that increases upon degradation and, consequently, absorb more water. After 8h the gelatin is almost fully degraded while Gel-*g*-PTMC$_6$ is disintegrated in several gel parts. In contrast, for the copolymer Gel-*g*-PTMC$_{10}$ a surface erosion behavior is noticed which seems to help the samples to maintain their physical integrity until total degradation. The kinetic of surface erosion is PTMC-dependent. Indeed, we observed that Gel-*g*-PTMC$_{16}$ degrades slowly with a slight start of erosion after 8h, whereas, Gel-*g*-PTMC$_{32}$ did not show any degradation in the time scale of the study. This last behavior is classically observed for crosslinked PTMC, which degradation mechanism relies mostly on enzymatic digestion.

3.6. Design and scaffold fabrication by stereolithography

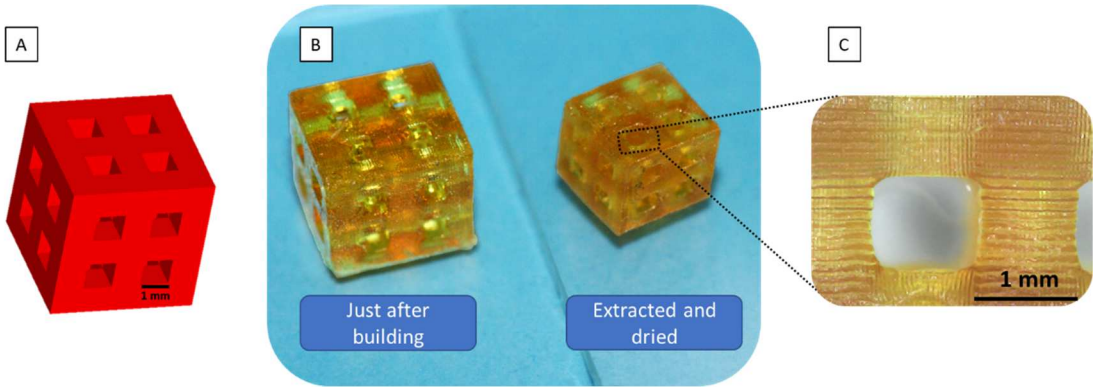

Figure 9. STL format of the designed scaffold (A), pictures of the SLA-produced 3D porous scaffold using Gel-*g*-PTMC$_{10}$ with different treatment conditions (B), and optical microscope view of the scaffold (C).

Finally, the photoreactivity of the hybrid polymers makes possible the resin to be used in additive manufacturing by vat photopolymerization. Gel-*g*-PTMC$_n$-MA was tested in SLA approach using a DLP apparatus. Having an appropriate resin viscosity is important to ensure efficient processability, and ideally, a resin viscosity around 1 to 10 Pa.s must be reached. Therefore, following the rheological

(Figure S1), the viscosities for Gel-*g*-PTMC$_n$ in DMSO at concentration 20% are much higher than the ideal viscosity for SLA. All the resins were then diluted in DMSO to reach a concentration of 40 wt%.

In order to demonstrate the potential of such hybrid resins to be processed in SLA we initially designed a squared scaffold with basic cubic porosity architectures (Figure 9A). 3D porous structures were successfully built by SLA, using all the Gel-*g*-PTMC$_n$-MA (Figure 9B). Pictures show the high performance of the fabrication with a remarkable respect of the fabrication compared to the initial STL file. The layer-by-layer pattern is visible in Figure 9C, with a layer thickness of approximately 100 µm. Finally, Figure 9B shows picture scaffolds just after building (left scaffold) and after DMSO extraction and drying (right scaffold). As 40% of DMSO was used to reach the appropriate viscosity for fabrication by SLA, the scaffold lost 33% of its initial volume after extraction and drying. This shrinking behavior is in correlation with previous studies with PTMC resins for SLA [6, 41]. One great advantage of our copolymers is the possibility to attain such high concentration and consequently, such high resin viscosity, which is a prerequisite for SLA fabrication.

PTMC has great potential to be used for TE strategy, which is highlighted by the numerous reports available in the literature [9]. One can nevertheless not forget to mention that, whenever a strong cell adhesion is needed, surface or bulk modification of PTMC polymer is needed. As a first proof of concept, we show that upon methacrylation, high resolution 3D porous scaffolds of Gel-*g*-PTMC$_n$ can be fabricated by SLA. Perspective works will be dedicated to further assess how the presence of gelatin moieties enhance the kinetic of cell adhesion within a scaffold.

4. CONCLUSION

Hybrid polymers Gel-*g*-PTMC$_n$ resulting from the grafting of synthetic biocompatible PTMC on natural gelatin were successfully achieved with a large range of properties regarding the length of the grafted PTMC. First, the challenging characterization of covalent association between synthetic and natural polymers was unlocked by a diffusion and a quantitative NMR spectroscopy approach considering the selective solubility of the precursors. Moreover, the ROP of TMC moiety from the gelatin was obtained with high monomer conversions and remarkable high yields. Secondly, homogeneous photo-crosslinking films based on Gel-*g*-PTMC$_n$ have shown promising mechanical

improvement with effective cytocompatibility and cells bioadhesion, independently of the chemical composition. The degradation study allows to decipher the key role of the PTMC in Gel-*g*-PTMC$_n$ copolymers, with a shift from bulk to surface degradation mechanism when increasing the ratio of PTMC. Impressively, all the Gel-*g*-PTMC$_n$-MA in solution led to appropriate viscosity while keeping a high degree of concentration in order to successfully build by SLA a well-defined 3D structure with high controlled porosity. These promising results open perspectives in the challenging field of hybrid polymer characterization and in the research of biomaterials adapted for additive manufacturing with suitable properties for tissue engineering application.

ASSOCIATED CONTENT

Supporting information

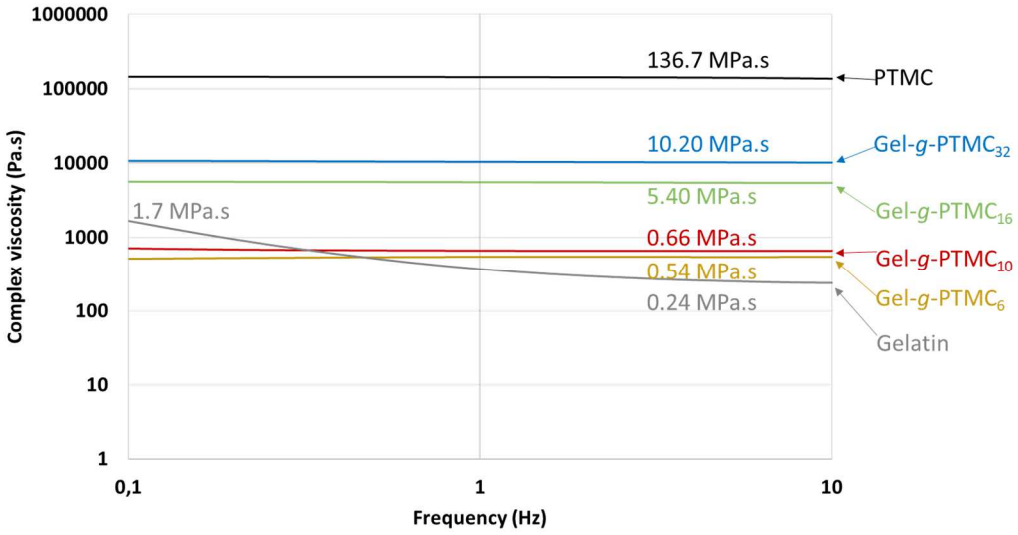

Figure S1. Complex viscosity *versus* frequency of native gelatin, pure PTMC and various Gel-*g*-PTMC$_n$ in DMSO (20 wt%).

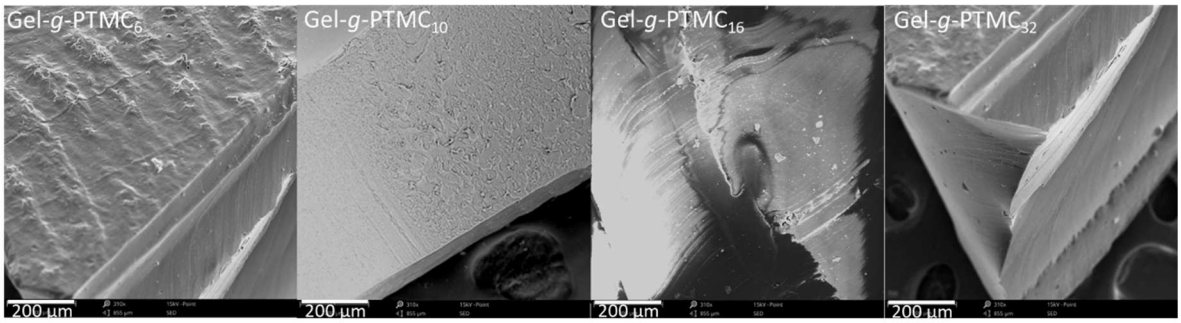

Figure S2. SEM images of cross-section photo-crosslinked Gel-g-PTMC$_n$ from low to high DP$_n$.

AUTHOR INFORMATION

Corresponding author

* Sebastien Blanquer ; sebastien.blanquer@umontpellier.fr

Author contribution

The manuscript was written through contributions of all authors. All authors have given approval to the final version of the manuscript.

Funding Sources

This work has been supported by the "Association Nationale Recherché et Technologie (ANRT)" and the company 3DMedlab.

AKNOWLEDGEMENT

The authors would like acknowledge the CARTIGEN platform (IRMB, CHU, Montpellier, France) for scanning electron microscopy facilities access, especially Dr. Mathieu Simon and Dr. Lucas Jego for helping with the pictures.

CONFLICT OF INTEREST

The authors declare no conflicts of interest.

REFERENCES

1. Jafari, M.; Paknejad, Z.; Rad, M. R.; Motamedian, S. R.; Eghbal, M. J.; Nadjmi, N.; Khojasteh, A., Polymeric scaffolds in tissue engineering: a literature review. *J Biomed Mater Res B* **2017,** *105* (2), 431-459.
2. Van Vlierberghe, S.; Dubruel, P.; Schacht, E., Biopolymer-Based Hydrogels As Scaffolds for Tissue Engineering Applications: A Review. *Biomacromolecules* **2011,** *12* (5), 1387-1408.
3. Guo, B. L.; Ma, P. X., Synthetic biodegradable functional polymers for tissue engineering: a brief review. *Sci China Chem* **2014,** *57* (4), 490-500.
4. Puppi, D.; Chiellini, F., Biodegradable Polymers for Biomedical Additive Manufacturing. *Appl Mater Today* **2020,** *20*.
5. Hsu, S. H.; Hung, K. C.; Chen, C. W., Biodegradable polymer scaffolds. *J Mater Chem B* **2016,** *4* (47), 7493-7505.
6. Guillaume, O.; Geven, M. A.; Varjas, V.; Varga, P.; Gehweiler, D.; Stadelmann, V. A.; Smidt, T.; Zeiter, S.; Sprecher, C.; Bos, R. R. M.; Grijpma, D. W.; Alini, M.; Yuan, H. P.; Richards, G. R.; Tang, T. T.; Qin, L.; Lai, Y. X.; Jiang, P.; Eglin, D., Orbital floor repair using patient specific osteoinductive implant made by stereolithography. *Biomaterials* **2020,** *233*.
7. van Bochove, B.; Hannink, G.; Buma, P.; Grijpma, D. W., Preparation of Designed Poly(trimethylene carbonate) Meniscus Implants by Stereolithography: Challenges in Stereolithography. *Macromol Biosci* **2016,** *16* (12), 1853-1863.

8. Blanquer, S. B. G.; Gebraad, A. W. H.; Miettinen, S.; Poot, A. A.; Grijpma, D. W.; Haimi, S. P., Differentiation of adipose stem cells seeded towards annulus fibrosus cells on a designed poly(trimethylene carbonate) scaffold prepared by stereolithography. *J Tissue Eng Regen M* **2017,** *11* (10), 2752-2762.
9. Fukushima, K., Poly(trimethylene carbonate)-based polymers engineered for biodegradable functional biomaterials. *Biomater Sci-Uk* **2016,** *4* (1), 9-24.
10. Vyner, M. C.; Li, A. N.; Amsden, B. G., The effect of poly(trimethylene carbonate) molecular weight on macrophage behavior and enzyme adsorption and conformation. *Biomaterials* **2014,** *35* (33), 9041-9048.
11. Asti, A.; Gioglio, L., Natural and synthetic biodegradable polymers: different scaffolds for cell expansion and tissue formation. *Int J Artif Organs* **2014,** *37* (3), 187-205.
12. Klimek, K.; Ginalska, G., Proteins and Peptides as Important Modifiers of the Polymer Scaffolds for Tissue Engineering Applications-A Review. *Polymers-Basel* **2020,** *12* (4).
13. Liu, X. H.; Holzwarth, J. M.; Ma, P. X., Functionalized Synthetic Biodegradable Polymer Scaffolds for Tissue Engineering. *Macromol Biosci* **2012,** *12* (7), 911-919.
14. Ullah, S.; Chen, X., Fabrication, applications and challenges of natural biomaterials in tissue engineering. *Appl Mater Today* **2020,** *20*.
15. Yi, S.; Ding, F.; Gong, L. I.; Gu, X. S., Extracellular Matrix Scaffolds for Tissue Engineering and Regenerative Medicine. *Curr Stem Cell Res T* **2017,** *12* (3), 233-246.
16. Levett, P. A.; Melchels, F. P. W.; Schrobback, K.; Hutmacher, D. W.; Malda, J.; Klein, T. J., A biomimetic extracellular matrix for cartilage tissue engineering centered on photocurable gelatin, hyaluronic acid and chondroitin sulfate. *Acta Biomater* **2014,** *10* (1), 214-223.
17. Klotz, B. J.; Gawlitta, D.; Rosenberg, A. J. W. P.; Malda, J.; Melchels, F. P. W., Gelatin-Methacryloyl Hydrogels: Towards Biofabrication-Based Tissue Repair. *Trends Biotechnol* **2016,** *34* (5), 394-407.
18. Echave, M. C.; Burgo, L. S.; Pedraz, J. L.; Orive, G., Gelatin as Biomaterial for Tissue Engineering. *Curr Pharm Design* **2017,** *23* (24), 3567-3584.
19. Comeau, P.; Willett, T., A Carbodiimide Coupling Approach for PEGylating GelMA and Further Tuning GelMA Composite Properties. *Macromol Mater Eng* **2021,** *306* (2).
20. Kushibiki, T.; Matsuoka, H.; Tabata, Y., Synthesis and physical characterization of poly(ethylene glycol)-gelatin conjugates. *Biomacromolecules* **2004,** *5* (1), 202-208.
21. Nie, K. X.; Han, S. S.; Yang, J. M.; Sun, Q. Q.; Wang, X. F.; Li, X. M.; Li, Q., Enzyme-Crosslinked Electrospun Fibrous Gelatin Hydrogel for Potential Soft Tissue Engineering. *Polymers-Basel* **2020,** *12* (9).
22. Hoch, E.; Hirth, T.; Tovar, G. E. M.; Borchers, K., Chemical tailoring of gelatin to adjust its chemical and physical properties for functional bioprinting. *J Mater Chem B* **2013,** *1* (41), 5675-5685.
23. Joy, J.; Aid-Launais, R.; Pereira, J.; Pavon-Djavid, G.; Ray, A. R.; Letourneur, D.; Meddahi-Pelle, A.; Gupta, B., Gelatin-polytrimethylene carbonate blend based electrospun tubular construct as a potential vascular biomaterial. *Mat Sci Eng C-Mater* **2020,** *106*.
24. Liang, J.; Grijpma, D. W.; Poot, A. A., Tough and biocompatible hybrid networks prepared from methacrylated poly(trimethylene carbonate) (PTMC) and methacrylated gelatin. *Eur Polym J* **2020,** *123*.
25. Dai, M.; Goudounet, G.; Zhao, H.; Garbay, B.; Garanger, E.; Pecastaings, G.; Schultze, X.; Lecommandoux, S., Thermosensitive Hybrid Elastin-like Polypeptide-Based ABC Triblock Hydrogel. *Macromolecules* **2021,** *54* (1), 327-340.
26. Zhang, Y.; Wu, K. Q.; Sun, H. L.; Zhang, J.; Yuan, J. D.; Zhong, Z. Y., Hyaluronic Acid-Shelled Disulfide-Cross-Linked Nanopolymersomes for Ultrahigh-Efficiency Reactive Encapsulation and CD44-Targeted Delivery of Mertansine Toxin. *Acs Appl Mater Inter* **2018,** *10* (2), 1597-1604.
27. Chartrain, N. A.; Williams, C. B.; Whittington, A. R., A review on fabricating tissue scaffolds using vat photopolymerization. *Acta Biomater* **2018,** *74*, 90-111.
28. Shirahama, H.; Lee, B. H.; Tan, L. P.; Cho, N. J., Precise Tuning of Facile One-Pot Gelatin Methacryloyl (GelMA) Synthesis. *Sci Rep-Uk* **2016,** *6*.
29. Brossier, T.; Volpi, G.; Lapinte, V.; Blanquer, S., Synthesis of Poly(Trimethylene Carbonate) from Amine Group Initiation: Role of Urethane Bonds in the Crystallinity. *Polymers-Basel* **2021,** *13* (2).
30. Claassen, C.; Claassen, M. H.; Truffault, V.; Sewald, L.; Tovar, G. E. M.; Borchers, K.; Southan, A., Quantification of Substitution of Gelatin Methacryloyl: Best Practice and Current Pitfalls. *Biomacromolecules* **2018,** *19* (1), 42-52.
31. Ovsianikov, A.; Deiwick, A.; Van Vlierberghe, S.; Dubruel, P.; Moller, L.; Drager, G.; Chichkov, B., Laser Fabrication of Three-Dimensional CAD Scaffolds from Photosensitive Gelatin for Applications in Tissue Engineering. *Biomacromolecules* **2011,** *12* (4), 851-858.
32. Stevens, P. V., Trace Bioorganic Constituents of Gelatins - a Review. *Food Aust* **1992,** *44* (7), 320-324.
33. Yue, K.; Li, X. Y.; Schrobback, K.; Sheikhi, A.; Annabi, N.; Leijten, J.; Zhang, W. J.; Zhang, Y. S.; Hutmacher, D. W.; Klein, T. J.; Khademhosseini, A., Structural analysis of photocrosslinkable methacryloyl-modified protein derivatives. *Biomaterials* **2017,** *139*, 163-171.

34. Toshikj, N.; Robin, J. J.; Blanquer, S., A simple and general approach for the synthesis of biodegradable triblock copolymers by organocatalytic ROP from poly(lactide) macroinitiators. *Eur Polym J* **2020,** *127*.
35. Li, X.; Mignard, N.; Taha, M.; Fernandez-de-Alba, C.; Chen, J. D.; Zhang, S. M.; Fort, L.; Becquart, F., Synthesis of Poly(trimethylene carbonate) Oligomers by Ring-Opening Polymerization in Bulk. *Macromol Chem Phys* **2020,** *221* (5).
36. Alba, A.; du Boullay, O. T.; Martin-Vaca, B.; Bourissou, D., Direct ring-opening of lactide with amines: application to the organo-catalyzed preparation of amide end-capped PLA and to the removal of residual lactide from PLA samples. *Polym Chem-Uk* **2015,** *6* (6), 989-997.
37. Anastasio, R.; Peerbooms, W.; Cardinaels, R.; van Breemen, L. C. A., Characterization of Ultraviolet-Cured Methacrylate Networks: From Photopolymerization to Ultimate Mechanical Properties. *Macromolecules* **2019,** *52* (23), 9220-9231.
38. Shin, H.; Olsen, B. D.; Khademhosseini, A., The mechanical properties and cytotoxicity of cell-laden double-network hydrogels based on photocrosslinkable gelatin and gellan gum biomacromolecules. *Biomaterials* **2012,** *33* (11), 3143-3152.
39. Pego, A. P.; Grijpma, D. W.; Feijen, J., Enhanced mechanical properties of 1,3-trimethylene carbonate polymers and networks. *Polymer* **2003,** *44* (21), 6495-6504.
40. Schuller-Ravoo, S.; Feijen, J.; Grijpma, D. W., Flexible, elastic and tear-resistant networks prepared by photo-crosslinking poly(trimethylene carbonate) macromers. *Acta Biomater* **2012,** *8* (10), 3576-3585.
41. Blanquer, S. B. G.; Werner, M.; Hannula, M.; Sharifi, S.; Lajoinie, G. P. R.; Eglin, D.; Hyttinen, J.; Poot, A. A.; Grijpma, D. W., Surface curvature in triply-periodic minimal surface architectures as a distinct design parameter in preparing advanced tissue engineering scaffolds. *Biofabrication* **2017,** *9* (2).